Rheologica Acta
https://doi.org/10.1007/s00397-025-01490-2

REVIEW

Powders and cohesive granular media: a rheological perspective

Olivier Pouliquen[1]

Received: 27 December 2024 / Revised: 24 March 2025 / Accepted: 24 March 2025

Abstract

This paper provides a rapid overview of the mechanics of cohesive granular materials and powders, with a particular focus on the development of constitutive equations for the steady flowing regime. We begin by reviewing the various sources of adhesion between particles, before exploring the onset of flow in cohesive materials. While yield conditions are central to many characterization methods, they provide limited insight into flow behavior. We then discuss recent studies on the flow of cohesive granular materials, emphasizing the development of constitutive equations. A direct comparison of results from DEM simulations across different studies highlights the importance of the interaction model details but reveals key insights into the relevance of different dimensionless numbers, paving the way for a more comprehensive rheological description of powders.

Keywords Granular media · Powders · Rheology · Cohesion

From granular materials to powders

Over the past two decades, significant efforts have been devoted to develop a rheological framework for understanding granular materials (Andreotti et al. 2013; Kasper et al. 2024). These materials, composed of collections of discrete grains, can be seen as a complex fluid, and understanding when and how they flow has vast implications in various applications, from industrial processes to geophysical phenomena. Recent developments on constitutive laws to describe granular flows rely on two fundamental observations (MiDi 2004). First, unlike suspensions, granular media are typically manipulated under conditions where the volume fraction is not directly controlled: for instance, when pouring sugar, the packing of grains has the freedom to dilate. The appropriate framework thus involves studying the material's response under imposed pressure rather than fixed volume. Practically, in a typical rheological setup, for example, in an annular shear geometry, this can be done by confining the granular material with a top plate free to move vertically while subjected to a fixed normal stress σ (Badetti et al. 2018). This means that the material is free to dilate when the shear rate is imposed.

The second key observation is that in the limit of rigid grains interacting through collisions and friction, there are no intrinsic timescales or force scales characterizing the interparticle interactions. This limits the number of dimensionless parameters needed to describe the system to a single one: the inertial number, which is the shear rate made dimensionless using the inertial time scale set by the confining pressure. This observation leads directly to the so-called $\mu(I) - \phi(I)$ rheology (MiDi 2004; da Cruz et al. 2005; Jop et al. 2006), where the granular flow is described by a friction law and a volume fraction law, which are functions of the inertial number only. Numerous experiments and simulation have shown that this $\mu(I) - \phi(I)$ rheology serves as a foundational, zero-order description of granular flows as shown in the seminal collective paper by GDR Midi (MiDi 2004). Based on this framework, progresses have been made to capture additional complexities in granular flows, such as dilatancy (Montella et al. 2021; Kasper et al. 2024), non-local effects (Bouzid et al. 2015; Kamrin 2019), and hysteresis phenomena (DeGiuli and Wyart 2017; Rocha et al. 2019; Mowlavi and Kamrin 2021). Today, our understanding of granular rheology is mature enough to address increasingly complex configurations, although important challenges remain open in the study of dry granular materials (Kamrin 2019).

In comparison, our understanding of the flow of powders, where particle sizes are small and interparticle forces such as van der Waals interactions, electrostatic forces, and

✉ Olivier Pouliquen
olivier.pouliquen@univ-amu.fr

[1] Aix Marseille University, CNRS, IUSTI, 5 rue Enrico Fermi, 13013 Marseille, France

capillary forces induced by humidity become significant, is far less advanced. The presence of attractive/adhesive inter-particle forces complicates flow behavior substantially, posing difficulties in processes such as storage transportation and handling. From a dimensional analysis point of view, the new inter-particle forces introduce new force or/and time scales, breaking the simplicity of dry granular materials. Although the powder technology community has developed extensive expertise on how to characterize and manipulate powders (Castellanos 2005; Shi et al. 2018), fundamental principles linking macroscopic properties to particle interactions remain largely unknown.

Originating from the granular media and suspensions community, we would like to explore in this paper to what extent the insights gained from dry granular materials can provide a foundation for advancing our fundamental understanding of powders. This paper presents a personal perspective, aiming to synthesize current knowledge of powder behavior, review diverse methodologies employed to study it, and assess the potential of a rheological framework inspired by recent progress in the understanding of dry granular materials. Our discussion is far from being exhaustive and is limited to the role of interparticle forces that stay identical during the flow, excluding considerations such as solid bridges or solubility effects that may arise in powders or very deformable particles. The focus is therefore on cohesive granular materials, although the term powders may be used in the following.

In the first section, we explore the various interparticle forces that contribute to adhesion, emphasizing the complexity and challenges in identifying the most relevant properties governing these interactions. The second section addresses the critical question of when a powder starts to flow, focusing on the concept of yield cohesive stress, a key bulk property. Many powder characterization methods rely on accurately measuring this yield stress. Finally, the third section discusses the challenge of describing powder flow, highlighting recent progress, primarily numerical, in developing constitutive laws for cohesive granular materials. One last remark is that throughout this paper, the term "adhesion" will be used to describe interactions at the particle scale, while "cohesion" will refer to the bulk property of the granular medium.

The origin of adhesion

The first challenge when trying to describe powder dynamics is understanding the diversity of particle interactions that may lead to cohesion. Investigating these particle-particle interactions is a research field on its own, which lies at the intersection between the physics of interfaces, tribology, mechanics, and chemistry (Maugis 2013). Identifying the key particle characteristics that govern the flow properties of powders is far from straightforward.

The different interactions

The first type of interaction to consider when dealing with small particles is the van der Waals interaction, which exists between any solid surfaces. Theoretical models have been developed to calculate the attractive forces between idealized smooth spherical particles, specifically under two limiting cases: soft particles (the JKR model Johnson et al. 1971) and rigid particles (the DMT model Derjaguin et al. 1975) (Fig. 1). In these frameworks, the adhesive force F_{adh} required to detach two contacting particles scales with the surface tension of the solid γ_s and the particle size d as $F_{adh} = \alpha \gamma_s d$. The proportionality constant α varies

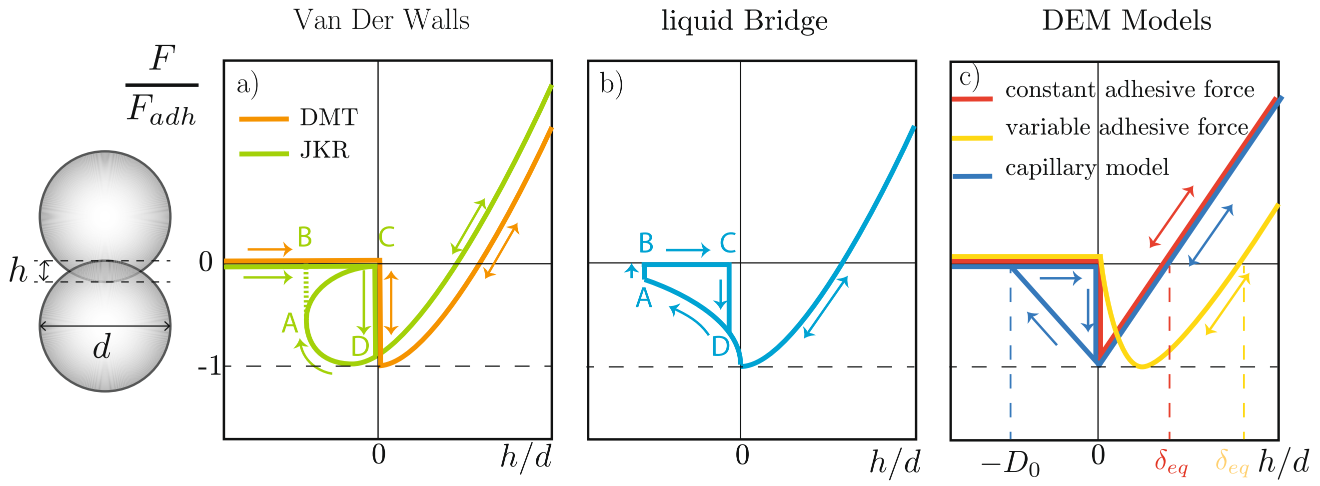

Fig. 1 Inter-particle interaction: force as a function of the particle distance h (positive when there is overlap) for different interactions; **a** van der Waals; **b** capillary bridge; **c** models used in DEM simulation (figure inspired by Fig. 1 of Rognon et al. (2008))

depending on whether the soft (JKR) or rigid (DMT) limit is considered. Figure 1a illustrates the force as a function of the distance between the particles for both soft and rigid cases, highlighting that, in the soft case, hysteresis occurs: detachment occurs when the force jumps from point A to point B and requires a finite separation distance, while attachment occurs upon direct contact ($C \rightarrow D$). It is crucial to note that the JKR model is highly sensitive to surface roughness due to its very short range (on the order of atomic distances). The force required to separate rough particles depends on the maximum compression force applied during contact, as this force determines the real contact area between the rough interfaces. Consequently, incorporating a JKR-like model into DEM simulations requires careful consideration of the interplay between surface roughness and contact forces (Abbasfard et al. 2016).

The second type of interaction commonly studied in powders is the presence of liquid between particles, leading to the formation of capillary bridges (Fig. 1b). In the bridge, the liquid is under low pressure, resulting in an attractive force (Halsey and Levine 1998; Herminghaus 2005; Mitarai and Nori 2006). Calculations for the ideal case of smooth particles show that the total adhesive force due to capillarity, when combined with van der Waals interactions, predicts the same force as the pure DMT van der Waals limit, i.e., a force proportional to the solid surface tension γ_s multiplied by the particle diameter d. This result implies that the amount of liquid in the capillary bridge does not change the adhesion, a somewhat counterintuitive outcome since it is well-known that a minimum amount of water is necessary to construct stable structures, such as a sandcastle. This paradox is solved considering the surface roughness of particles. At low liquid content, capillary bridges initially form between the tips of surface asperities, with their number increasing as the liquid content rises (Scheel et al. 2008). Consequently, adhesion increases until capillary bridge forms between the particles, beyond which the adhesive force saturates. Adding further liquid causes the capillary bridges to merge (funicular regime), reducing cohesion before the system reaches the fully immersed state. Figure 1b illustrates the variation of adhesive forces as a function of the distance between particles for a capillary bridge, demonstrating the presence of hysteresis: the distance required for detachment is controlled by the amount of liquid in the bridge ($A \rightarrow B$), while the bridge reforms only when particles are sufficiently close ($C \rightarrow D$).

In powders, ambient humidity plays a critical role in inducing adhesion between particles. While the adhesive force in this case is still attributed to capillary bridges, additional complexity arises due to the nucleation of the meniscus in a humid environment, a highly hysteretic phenomenon with an associated energy barrier for meniscus formation (Bocquet et al. 1998; Restagno et al. 2002). As a result, powders in humid environments often exhibit long-term evolution of their properties, a phenomenon commonly referred to as aging.

Another cause of complex interactions between particles is electrostatic interaction (Preudhomme et al. 2023). In air, particles can become charged during collisions and friction, a phenomenon known as triboelectricity. Understanding how charges are generated and distributed among the grains in an initially neutral assembly remains an open challenge. Recent experiments on single particles (Grosjean and Waitukaitis 2023) have revealed the dynamics of charge transfer, emphasizing the complexity of these interactions.

A last source of adhesion between particles worth mentioning is the presence of coatings on their surfaces. Coatings are commonly employed in industrial processes to modify surface properties. In particular, polymer coatings can act as reversible adhesives, introducing cohesion between particles. This technique has been proposed as a method to precisely control adhesion in model materials used in laboratory experiments (Gans et al. 2020, 2024). For example, by coating silica particles with polyborosiloxane (PBS), we have demonstrated the ability to finely tune the adhesive force between particles by simply varying the average thickness of the coating. Another techniques based on silanization of silica particles have been used to control adhesion between millimetric particles (Jarray et al. 2019). These methods enable the creation of short-range binary interactions that are reversible (particles can be detached and reattached, similar to a Post-it note) and controllable in a reproducible manner. Such a system serves as a proxy for powders, with the interaction range determined primarily by the thickness of the coating layer.

Given the wide range of particle interactions, different simplified models have been developed for discrete element method (DEM) simulations, as illustrated in Fig. 1c. The first model introduces a constant adhesive force added to the repulsive elastic force, which is linear for the sake of simplicity (red curve). A second model considers a variable force interaction, where the adhesive force increases with the square root of the overlap (yellow curve). Lastly, a family of models has been developed to mimic JKR model or capillary interactions (blue curve). These models account for a finite interaction length and incorporate hysteresis effects (Luding 2008; Roy et al. 2016).

In this brief overview of adhesive forces, we observe that while different types of adhesion share some common features, they also exhibit distinct characteristics İt remains unclear which contact parameters are most influential in determining the bulk properties of powders. The first and most widely discussed parameter is the detachment force, F_{adh}, which represents the force required to separate two particles in contact, a direct measure of the interaction strength.

A second important parameter is the interaction length or the typical distance at which the attractive force ceases to act. This length varies significantly depending on the type of interaction: it is on the order of the surface roughness size for van der Waals interactions, of the coating thickness for coated particles, and considerably larger for capillary bridges. Another critical parameter is the work required to detach two particles (Roy et al. 2016), typically given by the adhesion force multiplied by the displacement necessary for detachment. For short-range interactions, this displacement may involve contributions from particle deformation, when the elastic deformation is comparable to the interaction length. In this case, the stiffness of the particles becomes an important parameter (Mandal et al. 2020).

Finally, it is important to emphasize that the (macro) bulk properties of a granular packing are strongly influenced by dissipative interactions during the relative motion of particles. The interparticle dissipative properties can be significantly affected by the source of adhesion. For example, in the case of capillary bridges, if the fluid is highly viscous, it introduces additional dissipation during both normal and tangential displacement between particles (Vo et al. 2020; Kasper et al. 2021; Amarsid et al. 2024). Similarly, the presence of a liquid or a coating at the contact can act as a lubricant, drastically reducing the friction coefficient between particles.

To conclude this brief overview of particle interactions, it is important to note that their experimental characterization presents significant challenges. Most studies focus on measuring the adhesive detachment force. Various methods have been developed for this purpose. The general principle involves bringing two particles into contact, then pulling one away while tracking the force required for detachment. Force application can be achieved through centrifugation (Tran et al. 2021) or acceleration during an impact of a layer of grains deposit on a layer of glued particles (Deng et al. 2021) (interestingly this method gives access to the adhesive energy rather than the detachment force). Although these methods are not highly precise, they provide statistical data on detachment forces. The most reliable and precise method involves using an atomic force microscope (AFM). In this approach, one particle is fixed to the tip of a cantilever and brought into contact with another particle. This method also permits the measurement of friction coefficients. AFM techniques have been widely adopted in the suspension community for characterizing colloidal interactions (Comtet et al. 2017; Hsu et al. 2018, 2021), but their application to powders is still not common (Jones et al. 2003; Castellanos 2005; Fuchs et al. 2014).

When powders start to flow?

Before examining how powders flow, the first question to address is when they begin to flow, specifically, the yield stress. In this section, we first discuss the simple Mohr-Coulomb approach before introducing the concept of the flow function, which has been developed in the powder community to assess flow behavior in silos.

The cohesive Mohr-Coulomb criterion

A granular material can be seen as a yield stress fluid: a minimum stress is required for the grains to start flowing. In the absence of adhesive forces, dimensional analysis suggests that the onset of flow for a granular material confined under a stress σ (Fig. 2a) is governed, to a first approximation, by a Coulomb criterion. The yield stress, τ_{yield}, is proportional to the confining stress σ: $\tau_{yield} = \mu_s \sigma$, where $\mu_s = \tan \delta$ is the bulk friction coefficient and δ the friction angle. For materials like sand, the absence of external pressure thus implies no

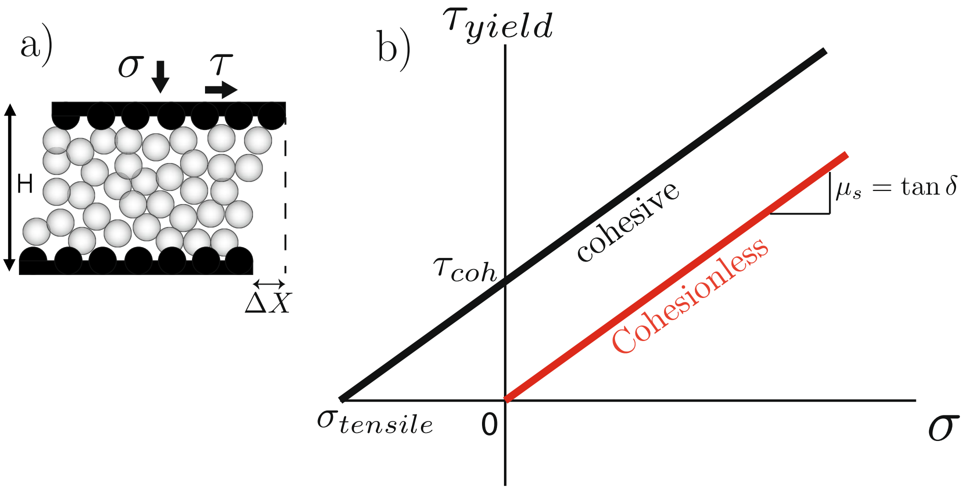

Fig. 2 **a** Sketch of the plane shear; σ is the prescribed vertical normal stress, τ the shear stress, H the thickness of the layer, and ΔX the displacement of the top plate relative to the initial position; **b** plastic yield criterion according to the Mohr-Coulomb plasticity model

yield stress, or equivalently, unconfined granular media can neither sustain tensile nor shear stresses.

However, this changes when adhesive forces are introduced between the grains. In powders, a yield stress can be measured even in the absence of external loading due to particle adhesion. Typically, the yield condition is expressed as $\tau_{yield} = \tau_{coh} + \mu_s \sigma$, where τ_{coh} represents the cohesive shear stress. The material can now sustain a tensile stress given by $\sigma_{tensile} = \tau_{coh}/\mu_s$ (see Fig. 2b). From dimensional arguments, we may assume that the cohesive stress is related to the typical adhesive force between particles at the origin of the cohesion F_{adh} divided by the characteristic surface area over which it acts d^2, where d is the particle diameter, meaning $\tau_{coh} \sim F_{adh}/d^2$.

A more precise estimate was first proposed by Rumpf (1958), who argued that particle interactions primarily induce an internal compressive stress, σ_{int}, as grains are attracted to one another. Assuming the material behaves like a Coulomb material, the yield condition becomes $\tau_{yield} = \mu_s(\sigma_{int} + \sigma)$, and the cohesive stress is equal to $\tau_{coh} = \mu_s \sigma_{int}$. In this simplified view, the internal compressive stress determines the magnitude of the tensile stress. From coarse graining arguments, the internal prestress can be estimated as Rumpf (1958); Richefeu et al. (2006); Badetti et al. (2018):

$$\sigma_{int} = \frac{3\phi Z F_{adh}}{2\pi d^2} \tag{1}$$

where ϕ is the volume fraction of the sample, and Z is the averaged number of contact per particle. This formula provides a good estimate of the cohesive stress (Richefeu et al. 2006). However, it has been shown in numerical simulations that the attractive forces between particles coupled with the finite range of the interactions might introduce additional contributions to the bulk cohesive stress (Badetti et al. 2018).

Measurement of the cohesive stress

Estimating the cohesive yield stress, τ_{coh}, is a crucial step for characterizing powders or cohesive materials (de Ryck et al. 2005; García-Triñanes et al. 2019). Various methods for determining τ_{coh} can be found in the literature, as summarized in Fig. 3. Some methods typically focus on measuring the tensile stress. One common approach involves measuring the flow through orifices of different sizes (Fig. 3a). The minimum diameter required for the material to flow provides an estimate of the tensile strength. Similarly, measuring the overhang that a layer of powder can sustain under gravity before it begins to break also offers insight into the tensile stress (Fig. 3b) (Raux and Biance 2018). Another method involves directly pulling on the material using split boxes designed to efficiently transmit the tensile stress (Fig. 3c). The inclined plane (Gans et al. 2020) is also used to measure the yield curve (Fig. 3d). By determining the critical angle at which a layer of material begins to flow and performing the experiment for different layer thicknesses, one can plot the relationship between shear stress and normal stress, from which the cohesive stress can be extracted. The most used techniques are based on linear or annular shear cells (Fig. 3e, f) (Shi et al. 2018; Schulze 2021). One measures the shear stress necessary to deform the material for different confining stresses, which allows the construction of the yield curve.

Role of the preparation

The discussion above does not consider the role of sample preparation. In dry cohesionless granular media, it is well known that an initially dense or loose sample exhibits different behaviors during quasi-static deformation, and both will reach a similar state only after a certain amount of

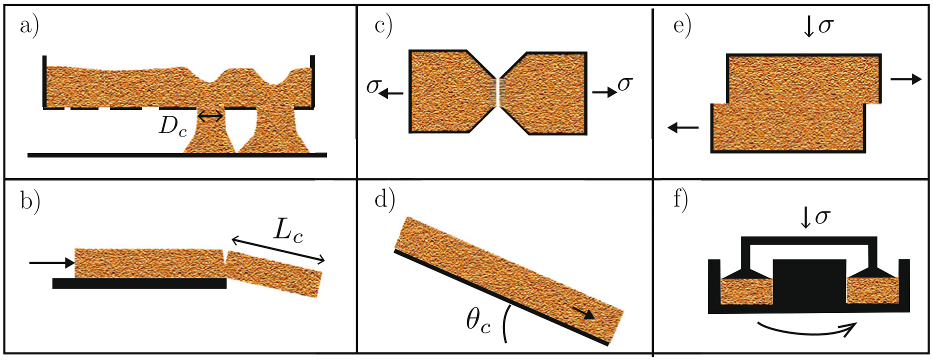

Fig. 3 Methods to measure the cohesive stress; **a** flow through different orifices, tensile strength is related to the size of the smallest orifice D_c with flow; **b** breakage of a layer of powders. Tensile stress is given by the critical length L_c when failure occurs; **c** split tensile box: the tensile strength is measured by pulling apart the two sides of a box full of powder; **d** inclined plane: by measuring the critical angle at which flow starts for different thicknesses provides the yield curve; **d** shear box; **e** annular shear cell

deformation. This role of sample preparation is even more pronounced in cohesive materials and powders.

Overconsolidated preparation Understanding how sample initial compaction influences the cohesive stress is central to a widely used technique developed to characterize the flowability of powders named the flow function (Carson and Wilms 2006; Shi et al. 2020a; Schulze 2021). This technique was initially proposed to characterize the resistance of a powder to start flowing in silos. It essentially involves measuring how cohesion varies with compaction. This definition of flowability differs from the powder's ability to flow, which we will discuss in the next section dedicated to rheology.

A typical measurement of the flow function is performed in a shear cell (Fig. 2a). The powder is first compacted in the shear cell under a maximum confining stress, σ_{max}. Usually in the preparation protocol, a pre-shear is imposed to get a reproducible initial preparation (Schulze 2021). The confinement is then reduced to a lower value σ_i to achieve an overconsolidated state, and the material is sheared quasi-statically by increasing the deformation $\gamma = \Delta X/H$ (Fig. 2a), while measuring the shear stress τ as a function of the deformation. The measurement is done for different confining stress σ_i (different colors in Fig. 4a) using the same preparation (grey curve in Fig. 4a). Figure 4a shows the typical behavior of shear stress τ as a function of deformation for different values of confining stress σ_i. The stress initially increases rapidly with increasing deformation, reaches a maximum, and then decreases, eventually reaching a steady value at large deformation. It is interesting to note that the behavior at large deformation in the steady state is not often discussed in the literature of powders (Louati et al. 2015), although this steady-state value is central to the theory of cohesionless granular materials in the context of critical state theory (Schofield and Wroth 1968). The reason is likely due to the development of shear banding or other inhomogeneities at large deformations for overconsolidated initial state, which make the interpretation of the steady state difficult.

The characterization of the flowability is based on measuring the peak value τ_{yield} for different confining pressures σ_i but under the same initial preparation under compression σ_{max}. Figure 4b shows a plot of τ_{yield} as a function of σ_i, with the arrow indicating for one case the stress path followed during the test. The yield curve, $\tau_{yield}(\sigma_i)$, can be fitted to find its intersection with the vertical axis at $\sigma = 0$, which provides the cohesive stress τ_{coh}. The slope of the curve gives the friction coefficient $\mu_s = \tan\delta$. Experimentally, the yield curve is often not perfectly linear as sketched in Fig. 4b, but instead exhibits a concave shape (Schulze 2021; Shi et al. 2020b). This experiment can be repeated for different values of the precompression σ_{max}, providing a set of yield curves (Fig. 4c). From these curves, we can deduce how the cohesive stress τ_{coh} evolves as the initial compression

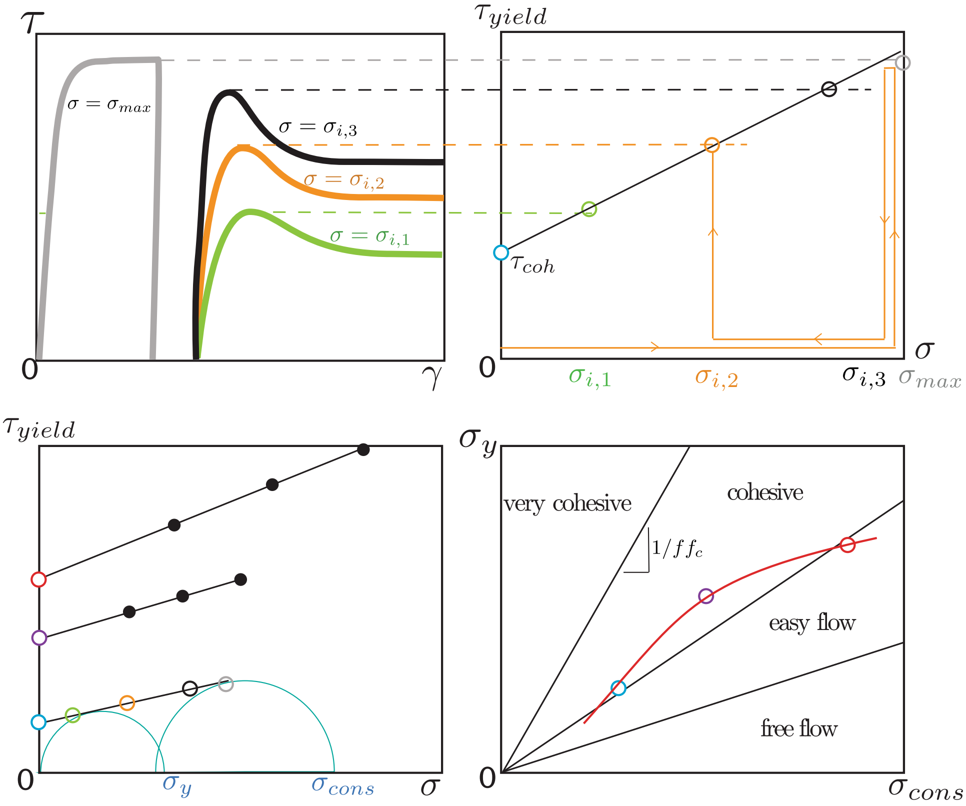

Fig. 4 How to measure the flow function of powders. **a** Shear stress τ versus deformation for different confining stresses σ_i after a preparation (grey curve) consisting in a pre-shear under normal stress σ_{max}. **b** Yield curve showing τ_{yield} at the peak as a function of σ_i. **c** Yield curves for different preparation stress level σ_{max}; the unconsolidated yield stress σ_y and the consolidation normal stress σ_{cons} are obtained from the two Mohr circles tangent to the yield curve passing through the origin for σ_y, through the last point for σ_{cons}; **d** σ_y as a function of σ_{consol}; the different lines correspond to different values of the flow index ff_c separating different flow regimes

σ_{max} increases. Traditionally, the flow curve is not directly $\tau_{coh}(\sigma_{max})$, but rather based on the unconfined yield stress σ_y (the stress at which the material would fail under a triaxial test with no external confining load) and the consolidation stress σ_{cons} (which is proportional to σ_{max}), both being constructed using the Mohr circle construction drawn (Fig. 4c) (see Schulze 2021). The relation $\sigma_y(\sigma_{cons})$ (or equivalently $\tau_{coh}(\sigma_{max})$) describes how cohesion varies with consolidation (Fig. 4d). If the increase in cohesion is slow, the material is expected to start to flow easily. If the increase is rapid, the powder is considered difficult to initiate flow. In the literature, the flow index ff_c is defined as the inverse of the slope of $\sigma_y(\sigma_{cons})$ and is intended to provide a quantitative measure of the "flowability" of a material: $ff_c < 2$ is supposed to mean very cohesive flows, $2 < ff_c < 4$ means cohesive flow, $4 < ff_c < 10$ means easy flowing, and $10 < ff_c$ means free flowing.

The main idea behind this widely used characterization technique is that a powder is considered easy to initiate flow if its cohesion does not increase significantly with increasing confining stress. However, this property named "flowability" does not inform about the flow properties, only its initiation. This observation motivates a deeper consideration of the rheology of these materials.

Underconsolidated preparation The approach described above, inspired by silo applications, focuses on the behavior of dense, compacted powders. However, the mechanics of fluffy and loose powder samples, which are of interest in phenomena such as snow avalanche dynamics, are less studied and mostly in discrete simulations. Uniaxial compression studies have shown the non-trivial role of sample preparation (Gilabert et al. 2008; Gaume et al. 2017). To reconcile underconsolidated and over-consolidated cases, a modified critical state theory taking into account cohesion has been developed. This theory describes the compaction and dilation occurring during transient shear flow of cohesive material, with applications to the description of snow avalanches (Gaume et al. 2018).

Dimensionless numbers

Before considering flow properties, it is important to emphasize that the cohesive stress discussed above, on its own, does not hold significant meaning. What matters is its comparison to the typical stresses developed in a given application. In the literature, several dimensionless numbers are introduced to compare τ_{coh} to other stresses. A first one is the Bond number, $Bo = \tau_{coh}/\rho_s g d$, which compares the pressure beneath a single grain under gravity to the cohesive stress. Equivalently, Bo is sometimes defined at the particle scale $Bo = F_c/mg$. A Bo value greater than unity indicates that the adhesive force is strong enough to hold two grains together under gravity. Another relevant dimensionless number is the cohesion number, $C = \tau_{coh}/\sigma$, which compares the cohesive stress to the typical confining pressure σ encountered in the application (or $C = F_{adh}/d^2\sigma$ when C is defined at the particle scale). Cohesion number greater than unity means that cohesive effects are expected to be important.

For example, in wet sand, the Bond number is greater than unity for particle diameters smaller than 1 mm. Considering a typical spoon full with 1 cm of wet grains of sand of diameter $d = 0.5$mm (Bo_{sand} 1) for which the cohesive stress is typically of order 100 Pa, the cohesion number is around $C \approx 0.3$. For flour, τ_{coh} is of the order of 1 kPa, meaning that the Bond number is of the order $Bo \approx 10^3$, and for a spoon of flour, the typical cohesion number is approximately $C \approx 10$.

In the next section, we discuss to which extent these dimensionless numbers can be useful in proposing constitutive laws for the flowing regime.

How powders flow?

Characterizing the flow properties of powders and understanding the origins of their flow difficulties is a challenging task, for which a rheological approach appears promising: the idea of applying a steady and uniform deformation rate to a powder and measuring the resulting stresses to derive constitutive laws is an approach that has been scarcely addressed in the literature (Rognon et al. 2008; Berger et al. 2016; Roy et al. 2017; Yamaguchi et al. 2018; Shi et al. 2020b; Mandal et al. 2021; Amarsid et al. 2024). While powder rheometers exist on the market, they typically measure macroscopic properties under more complex configurations than the plane shear, such as the torque exerted on a helical blade penetrating the medium (Freeman and Fu 2008) or the torque during the rotation of a vane (Bouillard et al. 2014). Other configurations like rotating drums are used (Alexander et al. 2006; Lumay et al. 2012; Jenkins et al. 2024), providing valuable and reproducible information about the flow behavior of weakly confined powders. These measurements are extremely useful for comparing different powders, but they do not yet enable the development of constitutive laws.

One of the major challenges in measuring the rheology of cohesive materials lies in the difficulty of shearing such media uniformly. Powders tend to localize deformation, forming shear bands. Additionally, controlling the cohesive properties of powders poses another significant experimental challenge. This difficulty in doing rheological experiments has initially driven the scientific community to adopt numerical approaches to tackle the question of rheology.

Towards constitutive laws for cohesive granular materials

Let us first consider the plane shear configuration theoretically, where the material is subjected to a constant shear rate $\dot{\gamma}$ under a confining stress σ. In the absence of adhesive forces and assuming rigid particles of size d and density ρ_s, dimensional analysis reveals that the shear stress τ and volume fraction ϕ, the two unknowns in this pressure-imposed configuration, depend only on the inertial number $I = \dot{\gamma} d/\sqrt{\sigma/\rho_s}$:

$$\tau = \mu(I)\sigma \quad \text{and} \quad \phi = \phi(I) \tag{2}$$

where $\mu(I)$ is an increasing function of I, starting at $\mu_s = \mu(0)$, representing the quasi-static friction coefficient discussed in "The origin of adhesion" section. On the other hand, $\phi(I)$ is a decreasing function of I, beginning at $\phi_c = \phi(0)$ in the quasi-static regime (i.e., the critical state), corresponding to the maximum volume fraction.

When an adhesive force F_{adh} is introduced between particles, we have seen in "Dimensionless numbers" section that a second dimensionless number, called the cohesive number $C = F_{adh}/\sigma d^2$, can be defined. This number compares the typical adhesive force between particles to the typical compressive force due to confinement. Cohesion is negligible at low values of C. Rognon et al. (2006, 2008) were the first to propose that the constitutive laws for such systems depend on both I and C, expressed as a friction law $\mu(I, C)$ and a volume fraction law $\phi(I, C)$. In the limit of small I and C, a linearization gives

$$\mu(I, C) \approx \mu_s + aC + bI \tag{3}$$

where the cohesive contribution aC and the inertial contribution bI add to the quasi-static friction coefficient μ_s. Consequently, the shear stress $\tau = \mu(I, C)\sigma$ can be expressed as

$$\tau = aF_{adh}/d^2 + (\mu_s + bI)\sigma \tag{4}$$

an equation consistent with the cohesive Mohr-Coulomb framework discussed in "The cohesive Mohr-Coulomb criterion" section, with the cohesive stress being equal to $\tau_{coh} = aF_{adh}d^2$. More generally, this approach of extending the $\mu(I)$ rheology to cohesive granular materials by simply adding a constant cohesive stress $\tau = \tau_{coh} + \mu(I)$ has been implemented in continuum simulations. These models have been validated against experimental measurements in configurations such as granular collapse (Staron et al. 2023; Gans et al. 2023) and silo flows (Gans et al. 2024), being able to capture some of the observed phenomena. This straightforward approach seems to perform reasonably well for systems with low cohesion. For larger cohesion levels, non-linear models have been proposed, based on a multiplicative correction instead of an additive correction by writing $\mu(I, C) = \mu(I) f(C)$ (Roy et al. 2017; Shi et al. 2020b).

Constitutive laws measured in DEM simulations

Several numerical studies have investigated the rheology of cohesive granular materials, aiming to understand how the friction coefficient and volume fraction evolve with the inertial number under different levels of cohesion (Khamseh et al. 2015; Berger et al. 2016; Yamaguchi et al. 2018; Badetti et al. 2018; Vo et al. 2020; Mandal et al. 2020; Macaulay and Rognon 2021; Amarsid et al. 2024; Roy et al. 2017). Most studies focus on the plane shear configuration where the shear is homogeneous, although inhomogeneous configurations might be used to infer a rheology if one have access to the local quantities (Shi et al. 2020b). However, comparing the results proves challenging. Some simulations are conducted in 2D, while others are in 3D, and the inter-particle interactions differ significantly across studies. Some employ capillary-like or JKR models, where attraction exists before contact over a finite interaction length accompanied by hysteresis between particle attachment and detachment. Others adopt simplified adhesive models, where the attractive force exists only at contact (Fig. 1c). Some used linear approximation for the force displacement in the elastic regime like in Fig. 1c; others used non-linear models.

Initially, there was hope that the details of inter-particle interactions would be negligible and that rheology would depend solely on the cohesion number C. However, a simple comparison reveals this is not the case. In Fig. 5, we have plotted the friction coefficient μ and volume fraction ϕ as functions of the inertial number I extracted from four studies (Khamseh et al. 2015; Berger et al. 2016; Mandal et al. 2021; Macaulay and Rognon 2021), based on both 3D and 2D simulations. Colors represent different cohesion numbers with similar values, while distinct symbols correspond to different studies. For the cohesionless case (shown in red), the measurements from different studies collapse onto a single curve, as expected. In contrast, the results for cohesive simulations vary significantly between studies. While all simulations show that increasing the cohesion number shifts the behavior toward higher friction coefficients and lower volume fractions, quantitative agreement is lacking, and qualitative trends differ. Some simulations exhibit a non-monotonic friction law, while others show monotonic behavior. This differences demonstrates that the cohesion number alone does not fully govern the rheology of cohesive granular materials, highlighting the critical influence of additional interaction parameters as observed in different studies.

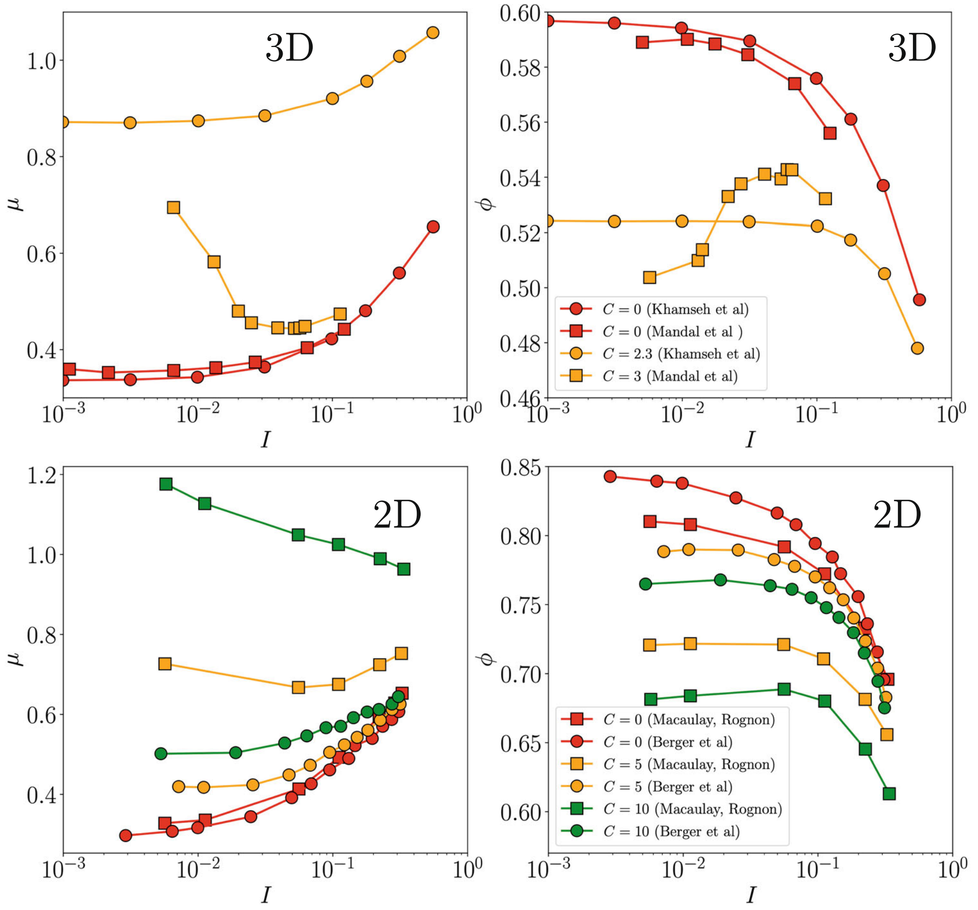

Fig. 5 The friction law $\mu(I)$ and volume fraction law $\phi(I)$ obtained in DEM simulations for different values of the cohesion number C, in 3D simulations from Mandal et al. (2021) and Khamseh et al. (2015), and 2D simulations from Berger et al. (2016) and Macaulay and Rognon (2021)

The case of adhesion with zero interaction length Let us first consider simulations using simplified interactions with zero interaction length, where the attractive force depends solely on particle overlap. In this case, Mandal et al. (2020, 2021) and Macaulay and Rognon (2021) demonstrated that, in addition to the attractive force, particle stiffness plays a significant role in determining the dynamics (The influence of particle inelasticity, which is less critical, will not be discussed here.) This finding contrasts with the cohesionless case, where rheology becomes independent of particle stiffness when the particles are sufficiently rigid (Silbert et al. 2001). When an adhesive force F_{adh} exists between particles, varying particle stiffness dramatically affects the material's bulk cohesion (Mandal et al. 2020, 2021). This effect is observed regardless of whether the normal contact force model is linear, defined by a spring constant k or Hertzian. For the same detachment force F_{adh}, stiff particles behave almost like cohesionless granular media, while softer particles exhibit strong cohesive behavior. In other words, the rigid limit does not seem to exist for attractive interactions with zero interaction length, contrary to the cohesionless case. However, this might no longer be true when the interaction range is non zero. These observations suggest that rheology is governed not only by the inertial number I and cohesion number C, but also by a third dimensionless parameter, the stiffness number K, defined as $K = \sigma d/k$, where σ is the confining pressure, d the particle diameter, and k the stiffness for a linear normal force model.

However, Mandal et al. (2020, 2021) demonstrated in their simulations that only two dimensionless numbers might be sufficient to describe the rheology, as the effects of cohesion and stiffness on the rheology can be combined into a single effective cohesion number, C_{eff}, defined as

$$C_{eff} = C\sqrt{\delta_{eq}/d}. \tag{5}$$

Here, δ_{eq} is the equilibrium overlap at which elastic deformation balances the attractive force ($\delta_{eq} = F_{adh}/k$ for a linear model). This relationship can also be expressed in terms of the other dimensionless numbers as $C_{eff} = C^{3/2}K^{1/2}$. When the adhesive force F_{adh} and stiffness k are varied while maintaining a constant C_{eff}, the flow properties remain the same, whether in plane shear or on an inclined plane (Mandal et al. 2020, 2021). This implies that the rheology is governed by a friction law $\mu(I, C_{eff})$ and a volume fraction law $\phi(I, C_{eff})$.

A simple explanation for this scaling can be provided by considering the work required to tangentially detach two particles with no external load. The work equals the tangential friction force $F_t = \mu_p F_{adh}$ multiplied by the typical sliding distance a needed to detach the particles. This sliding distance corresponds to the size of the contact zone, $a = \sqrt{\delta_{eq} d}$. Thus, the work is proportional to $\mu_p F_{adh}\sqrt{\delta_{eq}/d}$, explaining why C_{eff} as defined in Eq. 5 is the relevant parameter.

In 2D simulations, Macaulay and Rognon (2021) also proposed that the rheology depends on only two dimensionless parameters rather than three: the inertial number I and a cohesion energy number W. The parameter W compares the cohesion energy $F_{adh}\delta_{eq}$ to the typical kinetic energy of a particle moving with velocity $\dot{\gamma}d$, which is proportional to $\rho_p d^3 \dot{\gamma}^2 d^2$. The dimensionless cohesion energy number is defined as

$$W = \sqrt{\frac{F_{adh}\delta_{eq}}{\rho_p \dot{\gamma}^2 d^5}} = \frac{CK^{1/2}}{I}. \quad (6)$$

They proposed an empirical relation for the friction law in 2D, $\mu_{2D}(I, W)$. Interestingly, both this study and Mandal et al.'s work suggest that energetic arguments involving the energy required to detach particles are necessary for describing flow properties in addition to the detachment force. However, the scalings differ between the two studies, and more detailed analysis and comparison are necessary to better understand these differences.

The case of capillary-like interaction with finite interaction length When considering capillary-like interaction (Khamseh et al. 2015; Berger et al. 2016; Yamaguchi et al. 2018; Badetti et al. 2018; Vo et al. 2020; Amarsid et al. 2024), additional parameters come into play. In addition to the detachment force F_{adh}, to the stiffness k, there exists an interaction length D_0. Keeping the cohesion number $C = F_{adh}/\sigma d^2$ constant and decreasing the interaction length D_0 significantly decreases the friction coefficient, but has little influence on the volume fraction (Fig. 10 of Khamseh et al. (2015)). The work necessary to detach two particles being a function of D_0 (Roy et al. 2016), one can wonder if its influence might be similar to the influence of the stiffness discussed above for the case with zero-interaction length. Interestingly, the role of the adhesive energy has been underlined by Roy et al. (2016), who conducted simulations using two different adhesion models and found that the resulting flow is comparable only when the adhesive energy is kept constant between the two models.

Some recent simulations also incorporate viscous terms in their interaction models to account for dissipation in capillary bridges during relative motion between particles. The addition of viscosity shifts both the constitutive friction law and the volume fraction toward larger value of I (Fig. 4 in Amarsid et al. 2024). By analogy with work in suspensions, Vo et al. (2020) and Amarsid et al. (2024) demonstrated that the influence of the viscosity can be captured by defining a modified inertial number that incorporates the viscous timescale, thereby extending the applicability of the rheological framework to systems with significant viscous dissipation due to the interstitial liquid.

Existence of a shear-weakening branch

A critical point worth emphasizing in the discussion of cohesive material rheology, particularly from a simulation perspective, is the observation in several studies of a non-monotonic evolution in the constitutive bulk friction law. Studies such as those by Mandal et al. (2021) and Macaulay and Rognon (2021) (square symbols in Fig. 5) report that, at high levels of cohesion, the friction coefficient initially decreases with increasing inertial number I, reaches a minimum, and then increases again. Such non-monotonic constitutive laws are observed in other complex fluids and are known to be a source of instability (Olmsted 2008; Benzi et al. 2019; Divoux et al. 2016). In particular, numerous studies have shown that this shear-weakening behavior leads to localized deformation with the formation of shear bands. This observation of a non monotonic flow curve in cohesive granular materials could be highly significant, as it provides a potential explanation for why the flow of cohesive materials is often heterogeneous and opens new perspectives on interpreting the concept of flowability. An explanation for the occurrence of the unstable branch has been proposed by Macaulay and Rognon (2021), who describe the friction coefficient as the sum of two contributions: a quasi-static part that decreases continuously with increasing I, and an inertial part that increases with I.

To accurately capture this unstable branch, simulations must be conducted in small systems, typically less than eight particle diameters thick (Mandal et al. 2021). Decreasing the system size avoids the formation of shear bands, enabling the measurement of bulk rheology. One possible reason why this shear-weakening branch is not consistently observed across all numerical studies may be the use of systems that are too large, masking these behaviors. In large inhomogeneous systems, local measurements are required to accurately assess the rheology (Shi et al. 2020b). However, further research is necessary to clarify this point and determine the conditions under which this phenomenon emerges.

Microstructure

The relationship between microstructure and rheology has been extensively studied for dry granular materials. However, introducing adhesion between grains significantly alters particle organization during flow. Adhesion leads to less dense packing and the formation of clusters and aggregates

(Rognon et al. 2008; Roy et al. 2017; Amarsid et al. 2024), which are transient structures that influence stress transmission and momentum exchange. Several studies have examined the evolution of coordination numbers and the anisotropy of the contact network as adhesion increases. Yet, the exact role of the interaction law and the specific parameters of the adhesive force in controlling the microstructure and their connection to the differences in bulk rheology reported above remain unclear.

What about experiments?

Precise experiments aimed at measuring constitutive laws in shear cells for cohesive materials are limited (Klausner et al. 2000; Badetti et al. 2018; Amarsid et al. 2024). This reflects the significant challenges involved. Continuously shearing a thin layer of cohesive granular material under controlled normal stress, while maintaining control over adhesion, remains an open challenge in experimental rheology.

Amarsid et al. (2024) were among the first to present measurements of the friction law and volume fraction law for wet granular materials in a shear cell. In their experiments, cohesion was introduced by adding small quantities of silicon oil with varying viscosities. Their experimental data were compared to numerical simulations, which were calibrated to match the observations. However, the particle sizes used in their study resulted in relatively low cohesion levels in terms of the cohesion number ($C < 1$), limiting the exploration of strongly cohesive regimes.

Another experimental approach to infer the rheological properties of wet granular materials used the inclined plane configuration (Deboeuf and Fall 2023). By varying the inclination and flow rate and simultaneously measuring the flow thickness and velocity, the authors inferred an averaged friction law. Notably, their results showed that the data collapsed when using a cohesion length, rather than the particle diameter, in the definition of the inertial number I.

Finally, the rotating drum configuration, in which a cylinder partially filled with granular material is rotated, remains a simple and effective method for probing the influence of cohesion on granular flows (Jarray et al. 2019; Jenkins et al. 2024). However, extracting constitutive laws from the observed flow patterns remains a significant challenge (Hung et al. 2016).

Conclusion and perspectives

From this overview of the rheology of cohesive materials and powders, several conclusions emerge. First, cohesion in granular media is a complex phenomenon due to the diversity and complexity of attractive interparticle interactions that influence bulk material behavior. Second, the classical tools developed within the powder community, which are commonly used in industry to characterize powders, e.g., for silo design, focus primarily on plastic yield stress. These static measurements are of great interest, as they provide insight into the initiation of flow and compressibility of powders. However, the connection between these measurements and the material's flow properties remains unclear. Third, there is a clear need for a deeper understanding of the flowing regime of cohesive materials, both in steady and transient regimes. While the rheology of powders, in terms of constitutive equations, is still in its early stages, recent studies indicate that our knowledge of cohesionless granular materials provides a solid foundation for developing constitutive models for cohesive systems. In this effort, DEM simulations have proven to be a valuable tool. It is worth mentioning that, thanks to the increase in computational power, new methods have been developed where DEM is coupled with the finite element method. This approach properly describes the elasto-plastic deformation of particles and captures the evolution of cohesive forces at the contact points (Audry et al. 2024).

Although a direct comparison across studies is tricky due to the existence of different interaction models at the particle scale, one key message is that cohesive energy, rather than simply adhesive force, seems to be a crucial parameter influencing the dynamic properties of these materials. Clearly, experimental studies measuring the rheology of cohesive materials are still lacking. Applying continuous shear under controlled confining pressure to a cohesive granular material in a regime dominated by cohesion remains a challenge. A final remark is that in this paper, we focus on reviewing the deformation of cohesive materials under shear. However, cracks can also occur in cohesive materials, especially when extension is present during deformation (Géminard et al. 2012). Coupling rheology with the mechanics of crack propagation in a continuum description of cohesive granular materials is a challenge that has only recently been addressed (Blatny et al. 2024).

Acknowledgements Many thanks to Francisco M. Rocha for his careful reading of the manuscript. This work has benefited from fruitful discussions during our collaborative work on cohesive materials with Francisco M. Rocha, Denis Dumont, Vincent Bertin, Maxime Lajeunesse, Sandip Mandal, Adrien Gans, and Maxime Nicolas. Our study on cohesion has received funding from the European Research Council (ERC) under the European Union's Horizon (Grant 101097842, CohPa). The authors also acknowledge financial support from the International Fine Particle Research Institute (IFPRI) and the Agence Nationale de la Recherche under RheoCom (ANR-22-CE06-0020) grant.

References

Abbasfard H, Evans G, Moreno-Atanasio R (2016) Effect of van der Waals force cut-off distance on adhesive collision parameters in dem simulation. Powder Technol 299:9–18

Alexander AW, Chaudhuri B, Faqih A, Muzzio FJ, Davies C, Tomassone MS (2006) Avalanching flow of cohesive powders. Powder Tech 164(1):13–21

Amarsid L, Awdi A, Fall A, Roux JN, Chevoir F (2024) Viscous effects in sheared unsaturated wet granular materials. J Rheol 68(4):523–537

Andreotti B, Forterre Y, Pouliquen O (2013) Granular media between fluid and solid. Cambridge University Press, Cambridge

Audry N, Harthong B, Imbault D (2024) Numerical modelling of contact adhesion in a random assembly of elastic-plastic particles. Int J Solids Struct 295:112826

Badetti M, Fall A, Hautemayou D, Chevoir F, Aimedieu P, Rodts S, Roux JN (2018) Rheology and microstructure of unsaturated wet granular materials: experiments and simulations. J Rheol 62(5):1175–1186

Badetti M, Fall A, Chevoir F, Roux JN (2018) Shear strength of wet granular materials: macroscopic cohesion and effective stress: discrete numerical simulations, confronted to experimental measurements. Eur Phys J E 41(5):68

Benzi R, Divoux T, Barentin C, Manneville S, Sbragaglia M, Toschi F (2019) Unified theoretical and experimental view on transient shear banding. Phys Rev Lett 123(24):248001

Berger N, Azéma E, Douce JF, Radjai F (2016) Scaling behaviour of cohesive granular flows. Europhys Lett 112(6):64004–7

Blatny L, Gray J, Gaume J (2024) A critical state μ(I) -rheology model for cohesive granular flows. J Fluid Mech 997:67

Bocquet L, Charlaix E, Ciliberto S, Crassous J (1998) Moisture-induced ageing in granular media and the kinetics of capillary condensation. Nature 87:735–737

Bouillard J, Henry F, Marchal P (2014) Rheology of powders and nanopowders through the use of a Couette four-bladed vane rheometer: flowability, cohesion energy, agglomerates and dustiness. J Nanopart Res 16:1–17

Bouzid M, Izzet A, Trulsson M, Clément E, Claudin P, Andreotti B (2015) Non-local rheology in dense granular flows. Eur Phys J E 38(11):125

Carson JW, Wilms H (2006) Development of an international standard for shear testing. Powder Tech 167(1):1–9

Castellanos A (2005) The relationship between attractive interparticle forces and bulk behaviour in dry and uncharged fine powders. Adv Phys 4:263–376

Comtet J, Chatté G, Nigues A, Bocquet L, Siria A, Colin A (2017) Pairwise frictional profile between particles determines discontinuous shear thickening transition in non-colloidal suspensions. Nature Comm 8(1):15633

Cruz F, Emam S, Prochnow M, Roux J, Chevoir F (2005) Rheophysics of dense granular materials: discrete simulation of plane shear flows. Phys Rev E 72(2):021309

Deboeuf S, Fall A (2023) Cohesion and aggregates in unsaturated wet granular flows down a rough incline. J Rheol 67(4):909–909

DeGiuli E, Wyart M (2017) Friction law and hysteresis in granular materials. Proc Natl Acad Sci 114(35):9284–9289

Deng T, Garg V, Bradley M (2021) A study of particle adhesion for cohesive powders using a novel mechanical surface energy tester. Powder Tech 391:46–56

Derjaguin BV, Muller VM, Toporov YP (1975) Effect of contact deformations on the adhesion of particles. J Colloid Interface Sci 53(2):314–326

Divoux T, Fardin MA, Manneville S, Lerouge S (2016) Shear banding of complex fluids. Annu Rev Fluid Mech 48:81–103

Freeman R, Fu X (2008) Characterisation of powder bulk, dynamic flow and shear properties in relation to die filling. Powder Metall 51(3):196–201

Fuchs R, Weinhart T, Meyer J, Zhuang H, Staedler T, Jiang X, Luding S (2014) Rolling, sliding and torsion of micron-sized silica particles: experimental, numerical and theoretical analysis. Granular Matter 16:281–297

Gans A, Pouliquen O, Nicolas M (2020) Cohesion-controlled granular material. Phys Rev E 101:032904

Gans A, Abramian A, Lagrée PY, Gong M, Sauret A, Pouliquen O, Nicolas M (2023) Collapse of a cohesive granular column. J Fluid Mech 959:41

Gans A, Dalloz-Dubrujeaud B, Nicolas M, Aussillous P (2024) Discharge flow of a cohesive granular media from a silo. Phys Rev Lett 133(23):238201

García-Triñanes P, Luding S, Shi H (2019) Tensile strength of cohesive powders. Adv Powder Technol 30(12):2868–2880

Gaume J, Löwe H, Tan S, Tsang L (2017) Scaling laws for the mechanics of loose and cohesive granular materials based on Baxter's sticky hard spheres. Phys Rev E 96(3):032914

Gaume J, Gast T, Teran J, Herwijnen A, Jiang C (2018) Dynamic anticrack propagation in snow. Nature Comm 9(1):3047

Géminard J, Champougny L, Lidon P, Melo F (2012) Flexural fracturing of a cohesive granular layer. Phys Rev E 85(1):012301

Gilabert FA, Roux JN, Castellanos A (2008) Computer simulation of model cohesive powders: plastic consolidation, structural changes, and elasticity under isotropic loads. Phys Rev E 78(3):031305

Grosjean G, Waitukaitis S (2023) Single-collision statistics reveal a global mechanism driven by sample history for contact electrification in granular media. Phys Rev Lett 130(9):098202

Halsey T, Levine A (1998) How sandcastles fall. Phys Rev Lett 80(14):3141–3144

Herminghaus S (2005) Dynamics of wet granular matter. Adv Phys 54(3):221–261

Hsu CP, Ramakrishna SN, Zanini M, Spencer ND, Isa L (2018) Roughness-dependent tribology effects on discontinuous shear thickening. Proc Natl Acad Sci 115(20):5117–5122

Hsu CP, Mandal J, Ramakrishna SN, Spencer ND, Isa L (2021) Exploring the roles of roughness, friction and adhesion in discontinuous shear thickening by means of thermo-responsive particles. Nature Comm 12(1):1477

Hung CY, Stark CP, Capart H (2016) Granular flow regimes in rotating drums from depth-integrated theory. Phys Rev E 93(3):030902

Jarray A, Shi H, Scheper BJ, Habibi M, Luding S (2019) Cohesion-driven mixing and segregation of dry granular media. Sci Rep 9(1):13480

Jenkins BD, Nicuşan AL, Neveu A, Lumay G, Francqui F, Seville JPK, Weston D, Werner D, Windows-Yule CRK (2024) The sensitivity of powder characterization tool measurements to particle properties. Powder Technol 448:120231

Johnson KL, Kendall K, Roberts AD (1971) Surface energy and the contact of elastic solids. Proc R Soc Lond A 324(1558):301–313

Jones R, Pollock HM, Geldart D, Verlinden A (2003) Inter-particle forces in cohesive powders studied by AFM: effects of relative humidity, particle size and wall adhesion. Powder Technol 132(2):196–210

Jop P, Forterre Y, Pouliquen O (2006) A constitutive law for dense granular flows. Nature 441(7094):727–730

Kamrin K(2019) Non-locality in granular flow: phenomenology and modeling approaches. Front Phys 7

Kamrin K, Hill KM, Goldman DI, Andrade JE (2024) Advances in modeling dense granular media. Ann Rev Fluid Mech 56(1):215–240

Kasper JH, Magnanimo V, Jong SDM, Beek A, Jarray A (2021) Effect of viscosity on the avalanche dynamics and flow transition of wet granular matter. Particuology 59:64–75

Khamseh S, Roux JN, Chevoir F (2015) Flow of wet granular materials: a numerical study. Phys Rev E 92(2):022201–19

Klausner JF, Chen D, Mei R (2000) Experimental investigation of cohesive powder rheology. Powder Technol 112(1–2):94–101

Louati H, Oulahna D, Ryck A (2015) Apparent friction and cohesion of a partially wet granular material in steady-state shear. Powder Technol 278:65–71

Luding S (2008) Cohesive, frictional powders: contact models for tension. Granular Matter 10(4):235–246

Lumay G, Boschini F, Traina K, Bontempi S, Remy JC, Cloots R, Vandewalle N (2012) Measuring the flowing properties of powders and grains. Powder Technol 224((C)):19–27

Macaulay M, Rognon P (2021) Viscosity of cohesive granular flows. Soft Matter 17(1):165–173

Mandal S, Nicolas M, Pouliquen O (2020) Insights into the rheology of cohesive granular media. Proc Natl Acad Sci 117(15):8366–8373

Mandal S, Nicolas M, Pouliquen O (2021) Rheology of cohesive granular media: shear banding, hysteresis, and nonlocal effects. Phys Rev X 11(2):021017

Maugis D (2013) Contact, adhesion and rupture of elastic solids (Vol. 130). Springer Science & Business Media

MiDi G (2004) On dense granular flows. Eur Phys J E 14(4):341–365

Mitarai N, Nori F (2006) Wet granular materials. Adv Phys 55:1–45

Montella EP, Chauchat J, Chareyre B, Bonamy C, Hsu TJ (2021) A two-fluid model for immersed granular avalanches with dilatancy effects. J Fluid Mech 925:13

Mowlavi S, Kamrin K (2021) Interplay between hysteresis and nonlocality during onset and arrest of flow in granular materials. Soft Matter 17(31):7359–7375

Olmsted PD (2008) Perspectives on shear banding in complex fluids. Rheol Acta 47(3):283–300

Preudhomme N, Lumay G, Vandewalle N, Opsomer E (2023) Tribocharging of granular materials and influence on their flow. Soft Matter 19(45):8911–8918

Raux PS, Biance AL (2018) Cohesion and agglomeration of wet powders. Phys Rev Fluids 3(1):014301

Restagno F, Ursini C, Gayvallet H, Charlaix E (2002) Aging in humid granular media. Phys Rev E 66(2):021304

Richefeu V, El Youssoufi M, Radjai F (2006) Shear strength properties of wet granular materials. Phys Rev E 73(5):051304

Rocha FM, Johnson CG, Gray JMNT (2019) Self-channelisation and levee formation in monodisperse granular flows. J Fluid Mech 876:591–641

Rognon P, Roux JN, Naaim M, Chevoir F (2008) Dense flows of cohesive granular materials. J Fluid Mech 596:21–47

Roy S, Singh A, Luding S, Weinhart T (2016) Micro-macro transition and simplified contact models for wet granular materials. Comput Part Mech 3(4):449–462

Roy S, Luding S, Weinhart T (2017) A general(ized) local rheology for wet granular materials. New J Phys 19(4):043014–18

Rumpf H (1958) Grundlagen und methoden des granulierens. Chem Ing Tech 30(3):144–158

Ryck A, Condotta R, Dodds JA (2005) Shape of a cohesive granular heap. Powder Tech 157:72–78

Scheel M, Seemann R, Brinkmann MDMM, Di Michiel M, Sheppard A, Breidenbach B, Herminghaus S (2008) Morphological clues to wet granular pile stability. Nat Mater 7(3):189–193

Schofield AN, Wroth P (1968) Critical state soil mechanics vol. 310. McGraw-Hill London

Schulze D (2021) Flow properties of bulk solids, pp 57–100

Shi H, Mohanty R, Chakravarty S, Cabiscol R, Morgeneyer M, Zetzener H, Ooi JY, Kwade A, Luding S, Magnanimo V (2018) Effect of particle size and cohesion on powder yielding and flow. Kona Powder Part J 35:226–250

Shi H, Lumay G, Luding S (2020a) Stretching the limits of dynamic and quasi-static flow testing on cohesive limestone powders. Powder Technol 367:183–191

Shi H, Roy S, Weinhart T, Magnanimo V, Luding S (2020b) Steady state rheology of homogeneous and inhomogeneous cohesive granular materials. Granul Matter 22(1):1–20

Silbert LE, Ertaş D, Grest GS, Halsey TC, Levine D, Plimpton SJ (2001) Granular flow down an inclined plane: Bagnold scaling and rheology. Phys Rev E 64(5):051302

Staron L, Duchemin L, Lagrée PY (2023) Cohesive granular columns collapsing: numerics questioning failure, cohesion, and friction. J Rheol 67(5):1061–1072

Tran DT, Bittner R, Zámostnỳ P (2021) Adhesion force measurement by centrifuge technique as tool for predicting interactive mixture stability. Chem Eng Res Des 165:467–476

Vo TT, Nezamabadi S, Mutabaruka P, Delenne JY, Radjai F (2020) Additive rheology of complex granular flows. Nature Comm 11(1):1–8

Yamaguchi Y, Takada S, Hatano T (2018) Rheology of cohesive granular particles under constant pressure. J Physical Soc Japan 87(9):094802